

Preprint: Rapid estimation of climate-air quality interactions in integrated assessment using a response surface model

Sebastian D. Eastham^{1,2}, Erwan Monier^{2,3}, Daniel Rothenberg², Sergey Paltsev², Noelle E. Selin^{2,4,5}

¹Laboratory for Aviation and the Environment, Massachusetts Institute of Technology, Cambridge, MA 02139

²Joint Program on the Science and Policy of Global Change, Massachusetts Institute of Technology, Cambridge, MA 02139

³Land, Air and Water Resources, University of California Davis, Davis, CA 95616

⁴Institute for Data, Systems, and Society, Massachusetts Institute of Technology, Cambridge, MA 02139

⁵Department of Earth, Atmospheric, and Planetary Science, Massachusetts Institute of Technology, MA 02139

*Correspondence to: seastham@mit.edu

This is a non-peer reviewed preprint submitted to EartharXiv. It is being submitted for peer review at the journal ACS Environmental Au.

Rapid estimation of climate-air quality interactions in integrated assessment using a response surface model

Sebastian D. Eastham^{1,2}, Erwan Monier^{2,3}, Daniel Rothenberg², Sergey Paltsev², Noelle E. Selin^{2,4,5}

¹Laboratory for Aviation and the Environment, Massachusetts Institute of Technology, Cambridge, MA 02139

²Joint Program on the Science and Policy of Global Change, Massachusetts Institute of Technology, Cambridge, MA 02139

³Land, Air and Water Resources, University of California Davis, Davis, CA 95616

⁴Institute for Data, Systems, and Society, Massachusetts Institute of Technology, Cambridge, MA 02139

⁵Department of Earth, Atmospheric, and Planetary Science, Massachusetts Institute of Technology, MA 02139

*Correspondence to: seastham@mit.edu

Abstract

Air quality and climate change are substantial and linked sustainability challenges, and there is a need for improved tools to assess the implications of addressing them in combination. High-fidelity chemistry-climate simulations can capture combined climate-air quality responses to policy change, but computational cost has prevented integration of accurate air quality impacts into integrated assessment models (IAMs) used to inform policy development. Instead, IAMs often use global- or regional-scale marginal response factors to calculate air quality impacts of climate scenarios. To bridge this gap, we develop a computationally-efficient approach to quantify air quality impacts of combined climate and air quality interventions, capable of capturing spatial heterogeneity and complex atmospheric chemistry. We fit individual response surfaces to high-fidelity model simulation output for 1,525 locations worldwide under a variety of perturbation scenarios. Our intermediate-fidelity approach captures known differences in atmospheric chemical regimes, and can estimate location-by-location air quality under different scenarios within milliseconds. It can also be straightforwardly implemented in IAMs, enabling researchers to rapidly estimate how air quality in different locations, and related equity-based metrics, will respond to large-scale changes in emissions policy.

Using this approach we find that the sensitivity of air quality to climate change and air pollutant emissions reductions differs in sign and magnitude by region, suggesting that calculations of “co-benefits” of climate policy that do not account for the existence of simultaneous air quality interventions can lead to inaccurate conclusions. Although reductions in global mean temperature are effective in

improving air quality in many locations and sometimes yield compounding benefits, we show that the air quality impact of climate policy depends on air quality precursor emissions stringency.

Our approach can be extended to include results from higher-resolution modeling, but also to incorporate other interventions towards sustainable development which interact with climate action and have spatially-distributed equity dimensions.

1 Introduction

Air quality and climate are coupled problems, but are still typically managed separately. Despite a need for coordination to design more effective policies, much previous research to inform climate and air quality actions has focused on assessing interventions primarily designed to achieve either climate or air quality targets, while treating the other as a side-effect. Current modeling approaches are limited in their ability to simultaneously assess the implications of simultaneous emissions controls to reduce concentrations of harmful pollution, and climate policy that aims to reduce emissions of climate forcers such as greenhouse gases. Specifically, efforts to model the impacts of multiple intervention levers often sacrifice the detail needed to examine important distributional concerns. Here, we describe an approach that bridges the gap between integrated assessment modeling and full-scale atmospheric chemistry-climate simulations, and illustrate its application to address the impact of different policy levers on population exposure to health-damaging pollutants such as ozone and fine particulate matter (PM_{2.5}) in different global regions.

Researchers have used different approaches to assess the implications of climate policy on air quality. Climate policy will have direct air quality consequences, which are often quantified as the “climate penalty” of greenhouse gas emissions (Fiore, Naik, and Leibensperger 2015; Fu and Tian 2019). Much research also focuses on the “co-benefits” of climate action, taking the climate action as primary and air quality and other impacts as secondary (Garcia-Menendez, Monier, and Selin 2017; Garcia-Menendez et al. 2015). Recent work such as that by Hegwood et al. (2022) has questioned the framing of such “co-benefits”, as this implies a hierarchy of goals and priorities, and does not reflect the growing importance of justice and equity in the climate debate.

Studies which are instead focused on the potential impact of air quality interventions often use models to simulate a single change while holding all other factors constant, including climate change (Aleluia Reis et al. 2018; Rao et al. 2017). This can support efforts to identify what sort of air quality control would yield the greatest contribution to achieving an air quality target, but only as long as background conditions – including meteorology - remain approximately the same. Examples include estimating the contribution of individual power plants to US air pollution (Buonocore et al. 2014) or determining the air quality consequences of “excess” nitrogen oxide (NO_x) emissions from cars (Barrett et al. 2015). More generally, quantifications of the sensitivity of air quality to changes in different emissions can help to inform policy by indicating which interventions might be most effective (Dedoussi et al. 2020). There has also been work to assess how emissions changes motivated by air quality concerns could affect the climate, such as the effect of removing sulfur from ship fuel (Sofiev et al. 2018).

Recent work has argued for more coordinated climate and air quality efforts, recognizing both the presence of common sources and that the effect and effectiveness of emissions regulation will evolve with

a changing climate. Kinney (2021, 2018) and von Schneidmesser et al. (2020) have pointed out the need for more holistic consideration of air quality and climate policy. Some studies have used high-fidelity air quality models under different scenarios to directly compare the effects of air quality policy under different climate assumptions (Westervelt et al. 2019; Nguyen et al. 2020; Pommier et al. 2018; Nolte et al. 2018). These studies show greater air quality improvements are achievable through control of air pollutants than through avoidance of climate change in isolation, although factors such as the effect of temperature change on biogenic emissions (which can be ozone precursors) result in complex interactions. Other researchers have used integrated assessment models (IAMs) to provide rapid assessment of different scenarios, representing the effects of a broad slate of policy options on a range of relevant outcomes (Bosetti et al. 2006; Emmerling et al. 2019; van Soest et al. 2019; Nordhaus 2014; Nam et al. 2014). Although some IAMs focus on total economic impacts to inform quantities such as the Social Cost of Carbon (e.g. Nordhaus 2014), others have been used specifically to show greater health benefits from “welfare-maximizing policies” rather than a pure focus on climate policy (e.g. Reis, Drouet, and Tavoni 2022).

Existing efforts to better understand how air quality and climate policy together might affect environmental outcomes are currently limited by model capabilities and computational cost. Evaluating only select scenarios in detailed models (which is necessary because of the high computational cost of each scenario) can potentially result in misleading estimates of the effects of a policy choice. Jafino et al. (2021) discuss this in the context of adaptation policy, but the same is true when considering air quality policy. As an example, a future atmosphere might have greater marginal ozone production (per unit of NO_x emitted) than the current day. This counterintuitively implies that air quality policy will become “more effective”, even though the population’s exposure to ozone would be greater in absolute terms under any proposed NO_x control policy than would be the case for the present day. Additional complications arise if baseline ozone concentrations have also been affected by climate change. In contrast, integrated assessment approaches inherently rely on simplified representations of key atmospheric and economic processes to remain computationally tractable, and typically provide results at the scale of the global, regional, or national mean. However, the response of air quality to both climate and air quality policy is complex, with the same intervention (e.g. a decrease in NO_x emissions) sometimes having effects which vary in sign over the span of a few hundred kilometers. Regardless of the method used, focusing on global or regional mean responses can obscure the equity implications of climate and air quality policy.

Here, we describe an intermediate-fidelity approach which allows decision makers to understand and freely explore diverse scenarios of climate and air policy intervention – including their effects on equitability of outcomes – while minimizing the loss in accuracy. We do this by bridging between existing IAMs and chemistry-climate modeling. We use a full-complexity atmospheric chemistry-transport model which can accurately represent local chemical regimes to simulate global air quality under carefully-chosen climate and air pollutant emissions scenarios. By fitting a response surface to the results for each location across Earth, we produce a rapid assessment model which can estimate the effect of simultaneous changes in air pollutants and climate on air quality. Although such approaches have been used previously in modeling of air quality impacts alone (Heo, Adams, and Gao 2016), they have not to date been developed for climate-air quality interactions. This can facilitate assessment of multiple interventions that aim to reduce the health impact of air pollution. It also allows equity outcomes to be considered, since the response is independently characterized in each individual location rather than using

a global or regional mean. We then apply this approach to explore the challenge of achieving air quality goals under combined climate and air quality policy.

We first quantify the relationship between conventional air quality-relevant pollutants and outcomes, comparing our results to existing literature. We then use the same dataset to describe how interacting long-term (climate) and short-term (air quality) policies could affect our ability to achieve air quality targets in the future.

2 Methods

We perform a series of atmospheric chemistry simulations to project air quality under different climate and pollutant emissions scenarios (Paltsev et al. 2015) in the late 21st century. Using a global atmospheric chemistry model, we simulate air quality under two different climate scenarios, using five different realizations (ensemble members), and including perturbations to emissions of NO_x, SO_x, VOCs, and ammonia (five cases, including the baseline).

From these 50 simulations we fit response surfaces in every surface grid point with non-zero population, resulting in simplified models which allow us to evaluate the reductions in emissions which might be necessary to achieve air quality goals. For each combination of an outcome (e.g. surface ozone) and two levers or interventions (e.g. target global mean surface temperature (T) and NO_x emissions, or SO_x emissions and ammonia emissions) a separate surface is fitted in each location, ensuring that location-specific chemical regimes and responses are captured.

2.1 Methods: atmospheric modeling

We calculate surface air quality for a given combination of climate scenario and emissions perturbation using two linked models: the Community Atmosphere Model (CAM) v3.1, and a version of the GEOS-Chem High Performance (GCHP) regional-to-global air quality model which we modify to use meteorology generated by CAM.

Meteorological data for each climate projection are generated using CAM v3.1 as detailed by Monier et al. (2015), following scenarios “POL3.7” (3.7 W/m² in 2100, resulting in 1.1°C of warming in 2080-2100 relative to the 1990-2009 period) and “REF” (10 W/m², 4.3°C of warming) as described therein. This framework was evaluated in Monier et al. (2013) and found to produce a realistic simulation of observed climate trends. We use an ensemble approach, performing five different realizations using different sea surface wind stresses. Simulations are performed in CAM v3.1 at a global resolution of 2°×2.5°, on 26 vertical levels from the surface to a pressure of 2.2 hPa. To enable the use of this meteorology in GEOS-Chem, the same key variables are stored as are available from the NASA GMAO Modern Era Retrospective for Research and Analysis version 2 (MERRA-2) reanalysis dataset, and at the same temporal resolution. As a result, GCHP can be seamlessly switched between using meteorological data from MERRA-2 and from CAM.

Once meteorological data are available from CAM for each scenario realization, they are processed for use in GCHP. This approach means that emissions and meteorology can be decoupled in GCHP, allowing climate-focused and air quality-focused interventions to be assessed as separate levers. It also avoids

chaotic chemistry-climate feedbacks which would otherwise take decades to average out, but which do not fundamentally change the nature of the response. Surface-level concentrations of methane and CO₂ are prescribed in GCHP based on the appropriate climate projection. CO₂ is assumed to be uniformly distributed, while the distribution of surface methane concentrations is simulated by scaling spatially kriged observations from NOAA to provide the correct annual mean surface concentration (Murray 2016).

Global, anthropogenic emissions of all non-GHG species are prescribed based on the estimate for 2014 from the Community Emissions Data Set (CEDS) (Hoesly et al. 2018). Surface-level concentrations of long-lived species (other than CO₂ and methane) in GCHP are also prescribed for 2014, using existing emissions inventories. Emissions of biogenic species, soil NO_x, and sea salt are estimated during the simulation based on meteorological conditions for the given scenario and, in the case of biogenic emissions, on the scenario-specific CO₂ concentration. Emissions of lightning NO_x and mineral dust are prescribed based on a 2014 inventory for all simulation years.

Since GCHP is using a new source of meteorological data, we evaluate the skill of the model by comparing observed concentrations of surface ozone to that simulated using both the “standard” configuration and using the new meteorology. Figure S2 compares annual mean surface ozone between observational data (2010-2014, inclusive) from the TOAR-I dataset (Schultz et al. 2017a, 2017b) (<https://igacproject.org/activities/TOAR>) and values simulated using GCHP for 2014. We evaluate both the performance of a standard configuration of GCHP using meteorological data from the NASA Global Modeling and Assimilation Office the Modern Era Retrospective for Research and Analysis version 2 (GMAO MERRA-2) reanalysis, and using data from CAM. The MERRA-2 dataset was generated using the Goddard Earth Observation System (GEOS) model, and is one of two GEOS output datasets which are routinely used in assessments of air quality (Vohra et al. 2021; Potts et al. 2021; David et al. 2019; K. Li et al. 2019).

Considering the agreement between observed ozone and that simulated using MERRA-2 input (Figure S2, left panel) we find an r^2 of 0.23, a slope of 0.58, and a mean bias of 7.9 ppbv. The simulation using CAM data has an r^2 of 0.29, slope of 0.73, and mean bias of 15 ppbv, indicating a greater ability to represent differences between regions but a larger absolute error. Both simulations use identical emissions data. On the basis of these results we conclude that the model skill is not significantly degraded by the use of CAM meteorology compared to the use of GEOS meteorology. Parity plots, an evaluation of seasonal changes in model skill, the methods used to process the TOAR-I data, and an evaluation of model skill for wet deposition of sulfur and nitrogen are provided in the Supplemental Information.

2.2 Methods: fitting a response surface

For each location, we characterize the mathematical relationship between interventions (i.e. policy) and outcomes using data from the aforementioned CAM-GCHP simulations. Consider an environmental outcome which decision makers seek to achieve, such as a reduction in the ozone level in a single location. Any such quantity can be described as a function of long-term factors, short-term factors, and inherent uncertainty (chaos). Long-term factors include the total emissions of CO₂, N₂O, and CH₄ to date, and the subsequent changes in the global climate. Short-term factors include the local emissions of nitrogen oxides (NO_x), sulfur oxides (SO_x), and ammonia (NH₃), as well as the emissions in other

locations around the globe. The remaining factor is the chaotic nature of the atmosphere, resulting in uncertainty – typically expressed as a dependency on an initial condition. The model can therefore be expressed as

$$X = f(L_{i=1-N}, S_{j=1-M}, U)$$

where X is the objective quantity in some single location, L is a vector of N long-term factors, S a vector of M short-term factors, and U a variable representing the initial conditions. Members of each vector can reflect any input variable – including different species being emitted, different sectors or geographical source locations, or different times of the emission.

For many outcomes of climate change, the vector of long term factors might be approximated with a single scalar value. Since climate change is a global phenomenon with little sensitivity to the location of the cause (e.g. the location of CO_2 emissions), its effect in any given location can mostly be captured through a scalar such as the mean CO_2 equivalent mixing ratio, global radiative forcing, or global mean surface temperature. That reduces the model to

$$X = f(R, S_{j=1-M}, U)$$

where the vector L is now replaced with the scalar R . The left panel of Figure 1 illustrates how a conventional air quality study might then evaluate the effect of climate change on surface air quality through four simulations, where each simulation provides an estimate of X under different conditions. In this case U is neglected, assuming we are considering a single “realization” of the atmosphere.

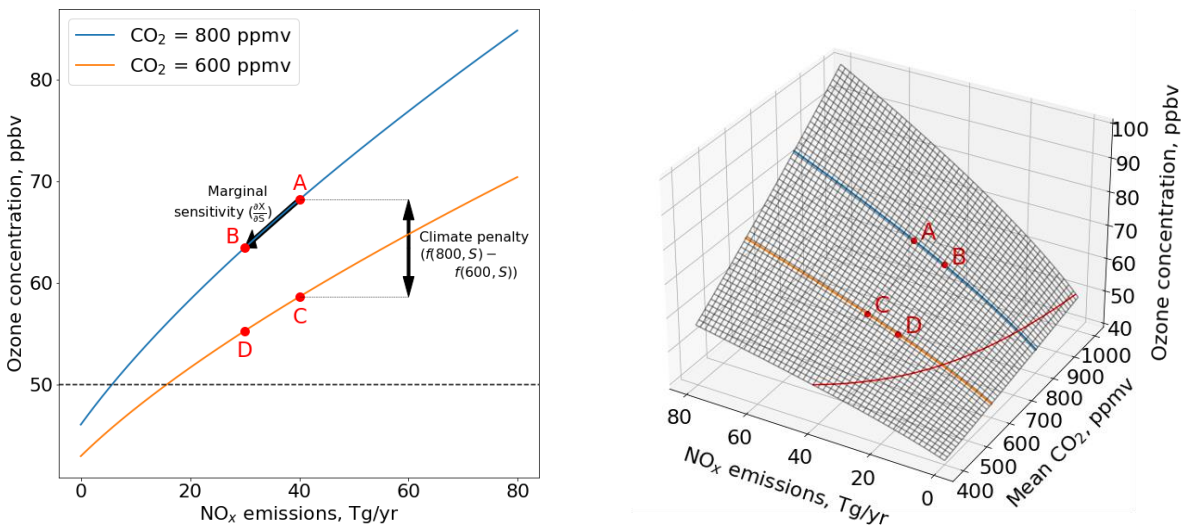


Figure 1. The response of surface air quality in one location to changes in air quality and climate policy. Left panel: a typical representation of how air quality policy (NO_x emissions stringency) might affect local air quality (ozone concentration) under two different climate policies (CO_2 levels). Right: a demonstration of how the two lines in the left panel are actually curves on the surface of a more general response plane, where a surface ozone response can be defined for any combination of climate and air quality policy. The red points in the right hand figure correspond to the results from individual simulations which can be used to develop a reduced-order estimate of the response surface.

For each climate scenario the full curve of possible results is shown, with each pair of simulations (A and B, C and D) providing the results for two scenarios along that curve. The figure also illustrates how each pair of results can be used to derive the marginal sensitivity of surface ozone to NO_x in each climate

scenario (dX/dS), while pairing A with C and B with D enables calculation of the climate penalty ($f(800,S) - f(600,S)$).

The effect of climate change on air quality can also be visualized as an intervention, or lever (i.e. an independent variable), in the same fashion as NO_x emissions, allowing their combined effect to be considered. The right panel of Figure 1 instead plots these four results as point estimates of a response surface. This recognizes that the effects of both dimensions (CO_2 and NO_x) on air quality are continuous. Furthermore, we can fit a two-dimensional response surface (most simply, a plane) to the four points. This allows us to gain insight into the response of our target variable for climate scenarios other than the two explicitly assessed by assuming linearity in the response. Although this introduces error, it exploits the broadly linear behavior of the atmosphere in response to perturbations. If we use global mean surface temperature in place of CO_2 or radiative forcing, this also frames the problem in terms of a common, physical target which is robust to uncertainty in (e.g.) climate sensitivity.

We use this approach to generate a response surface in each model grid point with non-zero population across Earth with respect to key climate and air quality emissions, resulting in a low-cost, intermediate-fidelity global air quality model. We calculate the response of ozone and $\text{PM}_{2.5}$ concentration across the world to changes in climate (expressed as a target global mean surface temperature T) and air quality emissions (NO_x , SO_x , VOCs, and ammonia). For each outcome and combination of two input variables (e.g. T and NO_x), we fit a response surface in each location which is described by three fit parameters (baseline value and gradient with respect to each parameter), producing a global model of air quality-climate interactions which can be applied in milliseconds.

2.3 Methods: experimental design

Data for fitting each response surface are generated using the GEOS-Chem High Performance (GCHP) (Eastham et al., 2018) chemistry transport model as described in Section 2.1. We use GCHP to simulate global air quality in the 2090s with year-2014 anthropogenic emissions of NO_x , SO_x , VOCs, and ammonia. The simulation is repeated four additional times, with a 10% reduction in global emissions of each pollutant (i.e. five simulations total). This exercise is performed for two different climate projections, consistent with a 2080-2100 mean warming (relative to 1990-2009) of either 1.1 or 4.3°C. The results of each simulated combination of surface temperature and air quality emissions are taken as the average result across all five realizations. The change in global mean surface temperature (ΔT) is used as the policy lever to represent climate change. This is consistent with its role in models such as DICE, which use global mean temperature as the key climate metric and calculate outcomes dependent on that target.

The result is a set of 10 data points describing the concentration of ozone (or $\text{PM}_{2.5}$) in each location globally under each climate projection and each air quality perturbation. For any set of two input variables (e.g. ΔT and NO_x emissions), a linear, 2-D response surface is fit to the relevant data points for each grid cell, producing a linearized model of the response of ozone (or $\text{PM}_{2.5}$) in that location to changes in both variables. If one of the two variables is ΔT , the fit is made to four points (e.g. 100% NO_x at 1.1°C, 90% NO_x at 1.1°C, 100% NO_x at 4.3°C, and 90% NO_x at 4.3°C). If both variables are air quality only, three points are used (e.g. 100% NO_x and VOCs, 100% NO_x and 90% VOCs, 90% NO_x and 100% VOCs) as combined reductions in air quality-relevant pollutants (“cross-terms”) are not simulated.

All simulations are performed for the period 2079-2099, with results stored hourly. The air quality response is calculated by averaging results from the period 2080-2099 to compensate for meteorological variability (Brown-Steiner et al. 2018), with the one-year period 2079-2080 discarded to avoid interference from transient “spin-up” effects. Simulations are performed at a global resolution of C24, roughly equivalent to $4^{\circ}\times 5^{\circ}$. Regional variations in air quality are therefore captured in response to global changes in climate and air quality precursor emissions.

2.4 Methods: quantifying and visualizing the effect of emissions reductions

Figure 2 shows how we fit the results from the simulations described above, where a response surface has been fit to the four points for a single location. We extrapolate or interpolate in areas where we have not explicitly calculated the response, indicated by a transition from opaque/blue to transparent/red in the figure. This fit is performed independently for each populated location on Earth, resulting in 1,525 independent fits of the response of ozone (or $PM_{2.5}$) to each combination of two input variables. Combined, these produce a model which can rapidly estimate the global, spatially-discretized response of air quality to combined changes in radiative forcing and air quality precursor emissions.

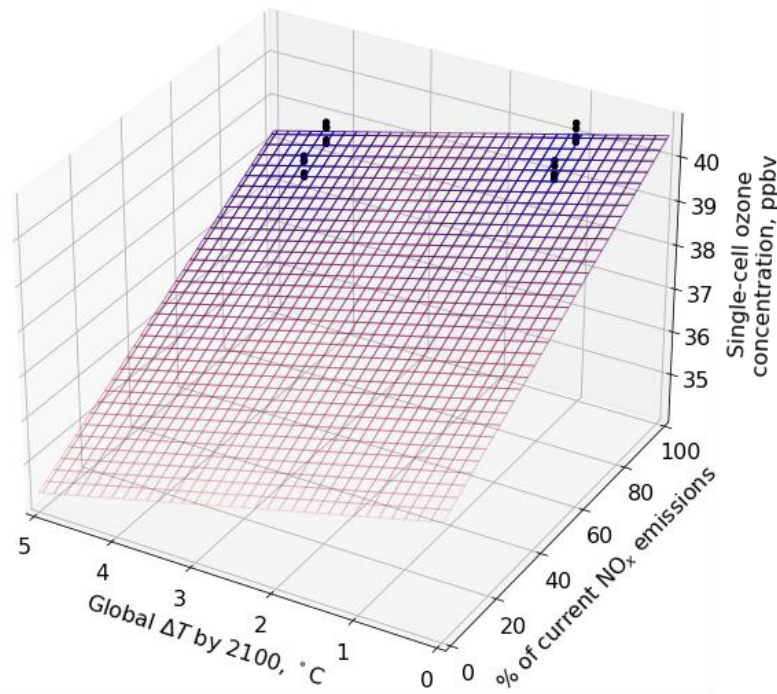


Figure 2. Demonstration of the fitting procedure. For each individual cell, we calculate the 20-year, five-member-ensemble outcome – in this case ozone concentration - for four different scenarios (black points). A plane is then fit through these 20 points to provide a linearized estimate of the local ozone response to changes in climate (represented by the change in global surface temperature) or emissions of (e.g.) NO_x . Colors indicate qualitatively where we are performing less (blue, solid) or more (red, faded) interpolation or extrapolation.

The use of a linear approximation is common in air quality calculations, as represented through marginal sensitivities (Dedoussi et al. 2020; Gilmore et al. 2019; Tessum, Hill, and Marshall 2017). Although the climate response to small perturbations is chaotic, atmospheric chemistry is broadly linear when examined at scale, or for small changes in emissions. However, large changes in either radiative forcing or emissions may result in substantial non-linearity which would not be captured when using a linear assumption (Raes et al. 2010). This could be addressed by calculating additional data points and using a non-linear fitting procedure.

2.5 Methods: application in this work

In our analysis, rather than quantifying the average surface ozone or $\text{PM}_{2.5}$ for each location under every combination of emissions, we instead quantify the fraction of a given population which would not be compliant with targets of either 50 ppbv maximum annual mean ozone exposure (MDA8, or maximum daily average over eight hours) or $8 \mu\text{g}/\text{m}^3$ annual mean $\text{PM}_{2.5}$ exposure. We refer to this quantity as the “population fraction with exposure above the target”. This approach reduces the risk of a low average value hiding inequities in population exposure.

To visualize this result, we use the response surfaces calculated for each model grid cell in a single region to determine whether the population in that location will be exposed to an ozone (or $\text{PM}_{2.5}$) concentration in excess of the target, for a given combination of two input variables (e.g. 10% reduction in NO_x emissions and a radiative forcing of $10 \text{ W}/\text{m}^2$). This is summed, weighted by population, across all grid cells in a given region to determine what fraction of the region’s population will be exposed to concentrations in excess of the target. By repeating this procedure while sweeping through possible combinations of input variables, an aggregate surface can be created which shows the fraction of the region’s population with exposure above the target, as a function of the input variables.

3 Results

We first use our approach to quantify the sensitivity of air quality to emissions of two short-lived pollutants under a “low-GHG” (1.1°C of warming and around 1,000 ppbv of background methane in 2100) future with year-2014 emissions of NO_x , VOCs, and other pollutants. Figure 3 shows how the population fraction in with exposure above the surface ozone target in four different regions (global, US, China, and the EU27) varies for different levels of VOC emissions, NO_x emissions, or both.

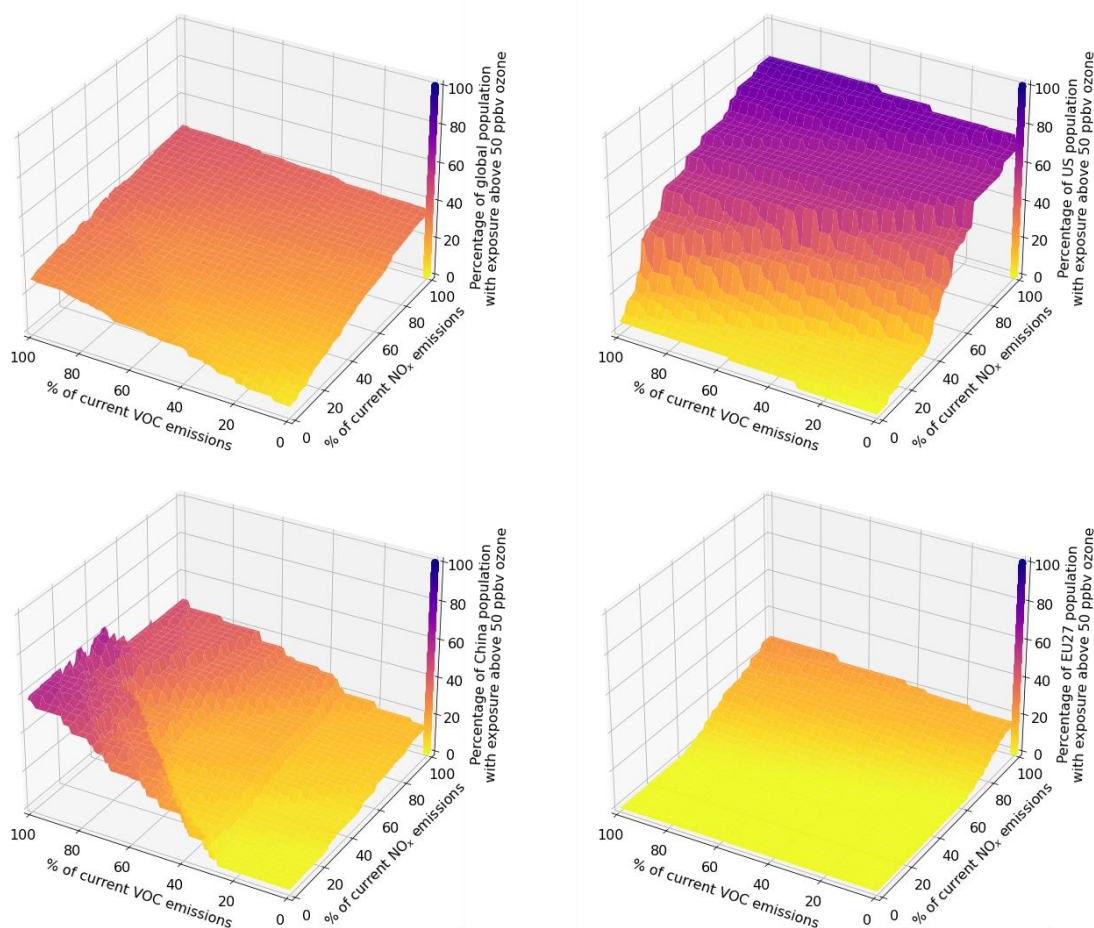


Figure 3. Response of surface ozone in 2080-2100 to reductions in VOC (x-axis) and NO_x emissions (y-axis). Results are shown in terms of the percentage of the target region population for whom exposure is above 50 ppbv. Different panels show different regions. Results are shown for a 2080-2100 warming of 1.1°C . Shading indicates the value on the vertical axis, as indicated by the color bar.

Reductions in either NO_x or VOC emissions consistently result in a reduction in the total population fraction with exposure above the target, together reducing the fraction from 44% to 3.9%. However, the response in individual regions is more complex. In China, we find that the atmosphere is predominantly NO_x saturated such that reducing NO_x emissions without any VOC controls increases the fraction above the target from 46 to 57%. However, reducing VOCs alone can reduce this to 14%, while combined NO_x and VOC reductions bring the fraction down to less than 1%.

In the US we find that lowering VOC emissions reduces the fraction of the population above the target exposure from 82% to 71%, but lowering NO_x emissions reduces the fraction to 36%. This indicates a NO_x -sensitive regime across most of the US for 2014-like emissions and conditions. Again, combined reductions ensure that both NO_x -sensitive and VOC-sensitive regions are addressed, resulting in the total population fraction with exposure above our target being reduced to 4.8%. As in China, our result does not capture a change in chemical regime, but rather reflects the fact that combined reductions in VOCs and NO_x allows ozone to be brought down regardless of the current chemical regime. Similar behavior is observed in the EU, where ozone levels are generally lower, and when aggregated globally.

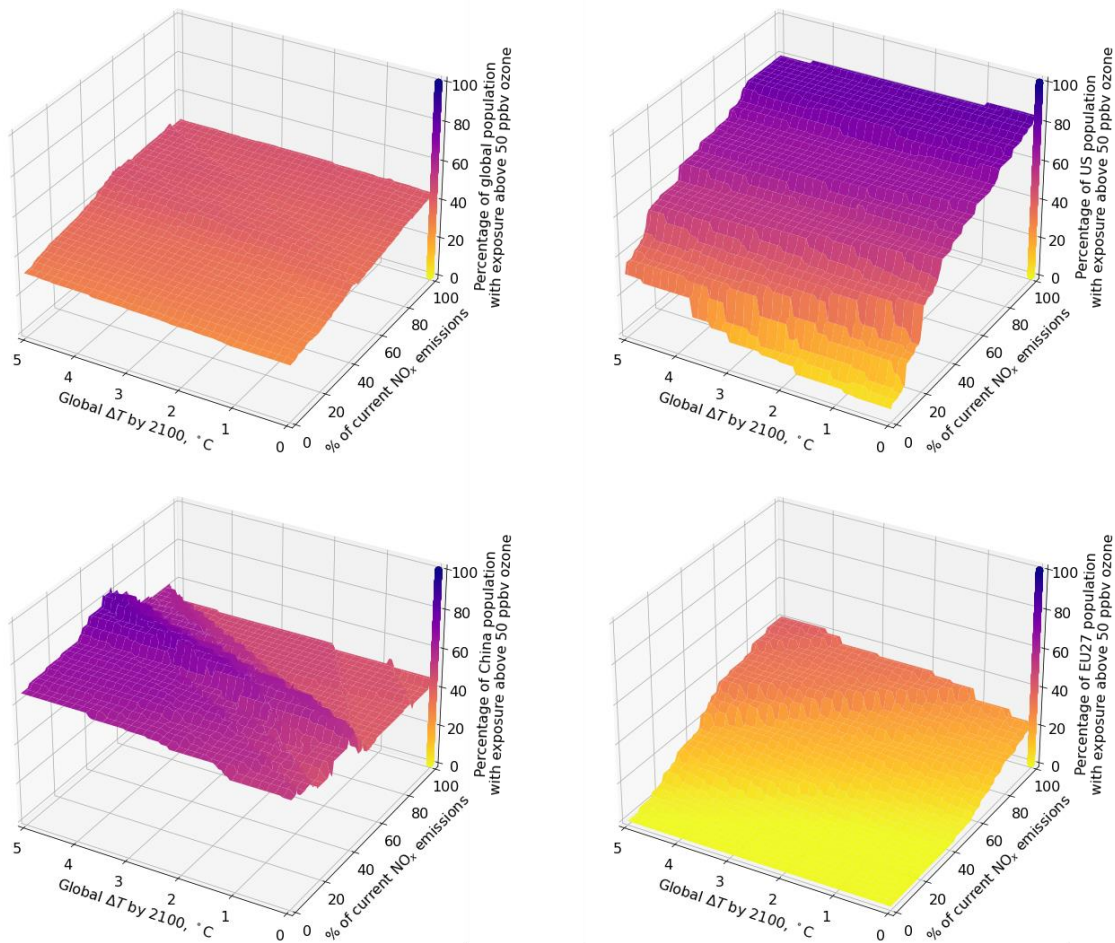


Figure 4. Response of surface ozone in 2080-2100 to reductions in future radiative forcing (x-axis) and NO_x emissions (y-axis). Results are shown in terms of the percentage of the target region population for whom exposure is above 50 ppbv. Different panels show different regions. Shading indicates the value on the vertical axis, as indicated by the color bar.

Figure 4 integrates climate change as an independent variable, showing how the fraction of the population above the target exposure level changes in response to reduced global warming and NO_x emissions in 2100 for the same four regions. Globally, we find a near-linear relationship between each independent variable and the population fraction with exposure greater than the given ozone target. Reducing the year-2080-2100 warming from 5 to 0°C reduces the fraction from 46 to 44%. Reducing NO_x emissions to zero while remaining at 5°C has a larger effect, dropping the fraction to 31%. Combined reductions in warming and NO_x emissions results in a small additional non-linear benefit, reducing the fraction to 27%. Similarly, reductions in either warming or NO_x emissions cause monotonic decreases in the population fraction above the target exposure for the EU27 region.

This linearity is not observed in all regions. For the US, reducing warming without any reduction in NO_x emissions results in a small increase in the population fraction above the target exposure, from 80% to 83%. This behavior reverses as NO_x emissions are reduced, and for zero NO_x emissions we find that reducing warming from 5 to 0°C reduces the fraction from 31 to 4.8%. In China, the relationship between

NO_x, and ozone is not monotonic, while reductions in warming produce only small improvements (4.8 to 12.5%) in the fraction of the population exposed to ozone levels above the target.

Figure 5 shows the response of anthropogenic PM_{2.5} to warming and ammonia (NH₃) emissions in the US and the EU27 region. In both regions, reducing ammonia emissions yields monotonically increasing reductions in the fraction of the population with exposure above the target. At high warming levels (5°C), 41% of the US and EU27 region populations are brought from above the target exposure to below it when ammonia emissions are reduced to 0%. However, in the EU27 region, a 5°C reduction in the target surface temperature results in a loss of sensitivity to ammonia emissions reductions. In China (not shown), the fraction above the target exposure remains at between 98.1 and 100% regardless of target surface temperature or NH₃ emissions level. Globally (not shown), 76% of the population have exposure greater than the target when ammonia emissions are reduced, compared to 85% for no reduction. The fraction is insensitive to temperature, falling from 85 to 84% as the target surface temperature change is reduced from 5 to 0°C.

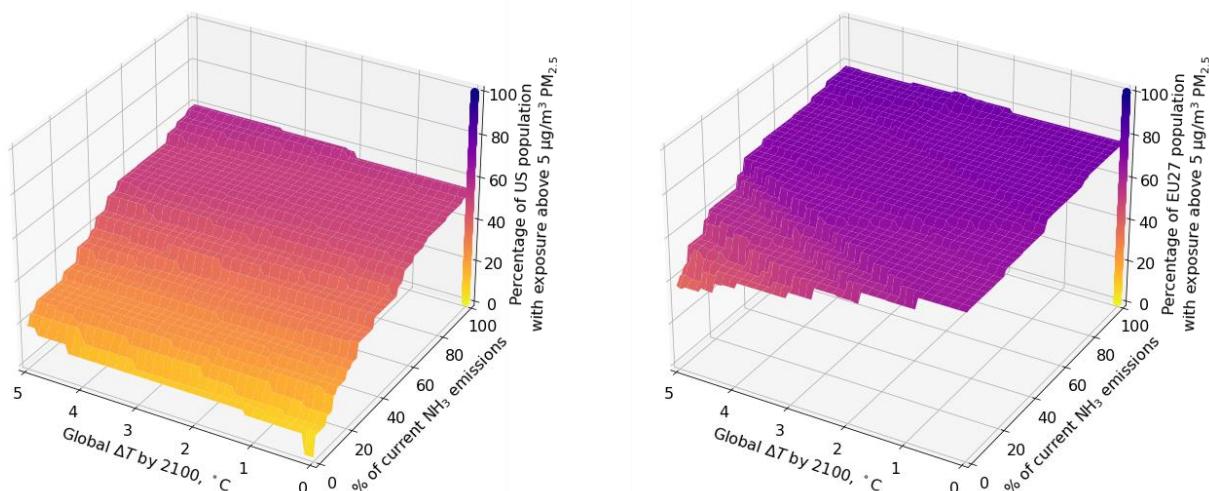


Figure 5. Response of surface anthropogenic PM_{2.5} in 2080-2100 to reductions in future radiative forcing (x-axis) and NO_x emissions (y-axis). Results are shown in terms of the percentage of the target region population for whom exposure is above 5 µg/m³. Different panels show different regions. Shading indicates the value on the vertical axis, as indicated by the color bar.

4 Discussion and conclusions

Our results for the sensitivity of air quality to reductions in NO_x and VOCs alone are consistent with current literature, indicating that the underlying model is appropriate for air quality assessments. Our analysis of the air quality response to NO_x and VOCs in China in a scenario with low background GHGs and near-current day pollutant emissions indicates that most regions are currently NO_x saturated, consistent with recent studies which have found NO_x controls in China to be ineffective in controlling ozone pollution (Chen et al. 2021). Similarly, the simulated response of US air quality to NO_x and VOCs shows NO_x-limited conditions rather than the NO_x-saturated conditions found in China. This is consistent with observed changes in the US chemical regime which are likely due to falling NO_x emissions and the relatively high concentration of biogenic VOCs (J. Li, Wang, and Qu 2019; Jung et al. 2022).

Using a spatially-disaggregated approach allows for different chemical regimes in one region to be captured in a rapid assessment model. In China, for example, we find a greater benefit for combined reduction of NO_x and VOCs compared to the sum of benefits from reducing each independently. This indicates the existence of a mix of VOC-sensitive and NO_x-sensitive regions, which could not be captured by approaches which treat the region and its air quality monolithically. The ability to represent spatial heterogeneity allows us to provide information on how to achieve benefits (or mitigate damages) for the largest possible population. With additional simulations, our approach could also indicate changes in the chemical regime which might occur at lower emissions levels.

These results indicate that our approach, despite being produced with a relatively coarse global model, is able to capture heterogeneity in the response of air quality to changes in emissions. Our method constitutes a reduced order approach to evaluate interactions between climate and air quality policy in terms of their impacts on public health. We assume linearity in the response of air quality to climate and air quality policy, and neglect interactions between pollutants in individual locations. However, by developing an independent fit of the response in every grid cell, our metric incorporates information on the differing chemical regimes across different locations. The results from work following this approach can be easily incorporated into integrated assessment models by providing three fit parameters for each location and outcome (ozone and PM_{2.5}), thereby advancing the ability of those models to represent the effects of climate and air quality policy on long-term air quality outcomes. Future work using higher-resolution modeling is expected to provide more granular information regarding the response of individual locations.

Differing sensitivities in different regions demonstrate the limitations of a co-benefits framing for climate-air quality interactions. Although reductions in global warming are effective in improving air quality in many locations and sometimes yield compounding benefits, our results show that the air quality co-benefit of climate policy is dependent on air quality precursor emissions stringency. The level of air quality benefit resulting from climate policy (reduced surface temperature change) relative to the benefit from air quality policy (reduced air quality precursor emissions) varies significantly by region, indicating that different regions will rationally prioritize different balances between climate and air quality policy. We also find that an air quality “co-benefit” of avoiding climate change is not inevitable, such as the increase in the fraction of the EU population exposed to high levels of PM_{2.5} with decreasing surface temperature. Our results support the need for holistic assessments of climate and air quality policy, and our approach provides an opportunity to perform such assessments.

In summary, this new approach enables rapid assessment modeling for air quality-climate interactions. We provided spatially-disaggregated ozone and PM_{2.5} estimates, splitting the global response into 1,525 independent subregions. For each region, we estimated the air quality response to policy which affects global surface temperature, air quality precursor emissions, or both. This enabled a first-order assessment of how climate and air quality policy might affect both the magnitude and distribution of air quality degradation worldwide within milliseconds, bridging the gap between integrated assessment modeling and high-fidelity chemistry-climate simulation.

The results shown here can be adapted to address several urgent, pertinent questions in the realm of climate and air quality interactions. This approach could be applied to estimate the integrated air quality impacts of any combined climate-air quality policy scenario on air quality outcomes, allowing decision

makers to understand how near- and mid-term air quality policy will be affected by a warming climate. This could include both evaluation of impacts and the identification of new policy options. Since the results of the approach are not tied to specific air quality or climate scenarios, a broader range of outcomes can be investigated than is possible with traditional single-scenario assessments.

There are several avenues to improve or extend our approach without increasing the number of simulations required. The use of a higher-resolution model would capture more granularity in the impacts on specific demographics, and better capture heterogeneity in chemical regimes. If the focus is on large reductions, it may be preferable to fit the response surface based on reductions in emissions which are greater than 10%, although this would then reduce the accuracy for smaller changes.

More generally, our method could be extended by performing additional simulations to develop a more complex response surface, effectively increasing the number of arguments considered in its functional form. The long-term factors could be separated so that surface warming and background methane concentrations are decoupled. Simulations with a simultaneous reduction in multiple variables could be used to determine “cross-terms” (e.g. with simultaneous reductions in VOCs and NO_x), or to explore further out in the parameter space (e.g. simulate 50 or 100% reduction in NO_x). A more complex paraboloid fit to these points in each location would allow changes in chemical regime to be captured. Finally, we consider only global changes in air quality emissions. Emissions scaling by location and/or by sector could enable evaluation of the impact of more targeted air quality policy under an uncertain climate future.

This approach can also be further extended beyond air quality outcomes. Although the data shown in this manuscript focus on interactions between climate policy (future global mean surface temperature) and air quality policy (emissions of NO_x, VOCs, and so on), our approach could equally be applied to investigate interacting air pollutants, or any other environmental policy question.

4.1 Acknowledgements

The MERRA-2 data used in this study/project have been provided by the Global Modeling and Assimilation Office (GMAO) at NASA Goddard Space Flight Center. Ozone observation data were acquired from the first phase of the Tropospheric Ozone Assessment Report (TOAR) initiative (<http://www.igacproject.org/activities/TOAR>). This publication was partially supported by the US EPA (grant no. RD-835872-01). Its contents are solely the responsibility of the grantee and do not necessarily represent the official views of the US EPA. Further, the US EPA does not endorse the purchase of any commercial products or services mentioned in the publication. This study was also supported by the Biogen Foundation.

4.2 Author contributions

NES conceived of the study and provided oversight. Development of the GCHP-CAM interface was performed by SDE with assistance from DR and EM. EM performed the CAM simulations. SDE performed GCHP simulations and analysis. SP provided EPPA input and developed the emissions matching scheme. SDE and NES produced the first draft of the manuscript collaboratively. All authors took part in manuscript edits and revisions.

4.3 Code and data availability

Configuration files to allow GCHP to use meteorological data from CAM are available upon request from the author, in addition to meteorological data for each climate realization.

4.4 References

- Aleluia Reis, Lara, Laurent Drouet, Rita Van Dingenen, and Johannes Emmerling. 2018. “Future Global Air Quality Indices under Different Socioeconomic and Climate Assumptions.” *Sustainability: Science Practice and Policy* 10 (10): 3645. <https://doi.org/10.3390/su10103645>.
- Barrett, S. R. H., R. L. Speth, S. D. Eastham, I. C. Dedoussi, A. Ashok, R. Malina, and D. Keith. 2015. “Impact of the Volkswagen Emissions Control Defeat Device on US Public Health.” *Environmental Research Letters* 10. <http://iopscience.iop.org/article/10.1088/1748-9326/10/11/114005/meta>.
- Bosetti, Valentina, Carlo Carraro, Marzio Galeotti, Emanuele Massetti, and Massimo Tavoni. 2006. “WITCH A World Induced Technical Change Hybrid Model.” *Energy Journal* 27: 13–37. <http://www.jstor.org/stable/23297044>.
- Brown-Steiner, Benjamin, Noelle E. Selin, Ronald G. Prinn, Erwan Monier, Simone Tilmes, Louisa Emmons, and Fernando Garcia-Menendez. 2018. “Maximizing Ozone Signals among Chemical, Meteorological, and Climatological Variability.” *Atmospheric Chemistry and Physics* 18 (11): 8373–88. <https://doi.org/10.5194/acp-18-8373-2018>.
- Buonocore, Jonathan J., Xinyi Dong, John D. Spengler, Joshua S. Fu, and Jonathan I. Levy. 2014. “Using the Community Multiscale Air Quality (CMAQ) Model to Estimate Public Health Impacts of PM_{2.5} from Individual Power Plants.” *Environment International* 68 (July): 200–208. <https://doi.org/10.1016/j.envint.2014.03.031>.
- Chen, Xiaokang, Zhe Jiang, Yanan Shen, Rui Li, Yunfei Fu, Jane Liu, Han Han, et al. 2021. “Chinese Regulations Are Working—Why Is Surface Ozone over Industrialized Areas Still High? Applying Lessons from Northeast US Air Quality Evolution.” *Geophysical Research Letters* 48 (14). <https://doi.org/10.1029/2021gl092816>.
- David, Liji M., A. R. Ravishankara, Jared F. Brewer, Bastien Sauvage, Valerie Thouret, S. Venkataramani, and Vinayak Sinha. 2019. “Tropospheric Ozone over the Indian Subcontinent from 2000 to 2015: Data Set and Simulation Using GEOS-Chem Chemical Transport Model.” *Atmospheric Environment* 219 (December): 117039. <https://doi.org/10.1016/j.atmosenv.2019.117039>.
- Dedoussi, I. R., S. D. Eastham, E. Monier, and S. R. H. Barrett. 2020. “Premature Mortality Related to United States Cross-State Air Pollution.” *Nature*.
- Emmerling, Johannes, Laurent Drouet, Kaj-Ivar van der Wijst, Detlef van Vuuren, Valentina Bosetti, and Massimo Tavoni. 2019. “The Role of the Discount Rate for Emission Pathways and Negative Emissions.” *Environmental Research Letters: ERL [Web Site]* 14 (10): 104008. <https://doi.org/10.1088/1748-9326/ab3cc9>.

- Fiore, Arlene M., Vaishali Naik, and Eric M. Leibensperger. 2015. "Air Quality and Climate Connections." *Journal of the Air & Waste Management Association* 65 (6): 645–85. <https://doi.org/10.1080/10962247.2015.1040526>.
- Fu, Tzung-May, and Heng Tian. 2019. "Climate Change Penalty to Ozone Air Quality: Review of Current Understandings and Knowledge Gaps." *Current Pollution Reports* 5 (3): 159–71. <https://doi.org/10.1007/s40726-019-00115-6>.
- Garcia-Menendez, Fernando, Erwan Monier, and Noelle E. Selin. 2017. "The Role of Natural Variability in Projections of Climate Change Impacts on U.S. Ozone Pollution: Natural Variability in Ozone Projections." *Geophysical Research Letters* 44 (6): 2911–21. <https://doi.org/10.1002/2016GL071565>.
- Garcia-Menendez, Fernando, Rebecca K. Saari, Erwan Monier, and Noelle E. Selin. 2015. "U.S. Air Quality and Health Benefits from Avoided Climate Change under Greenhouse Gas Mitigation." *Environmental Science & Technology* 49 (13): 7580–88. <https://doi.org/10.1021/acs.est.5b01324>.
- Gilmore, Elisabeth A., Jinhyok Heo, Nicholas Z. Muller, Christopher W. Tessum, Jason D. Hill, Julian D. Marshall, and Peter J. Adams. 2019. "An Inter-Comparison of the Social Costs of Air Quality from Reduced-Complexity Models." *Environmental Research Letters: ERL [Web Site]* 14 (7): 074016. <https://doi.org/10.1088/1748-9326/ab1ab5>.
- Hegwood, Margaret, Ryan E. Langendorf, and Matthew G. Burgess. 2022. "Why Win–Wins Are Rare in Complex Environmental Management." *Nature Sustainability*, March, 1–7. <https://doi.org/10.1038/s41893-022-00866-z>.
- Heo, Jinhyok, Peter J. Adams, and H. Oliver Gao. 2016. "Reduced-Form Modeling of Public Health Impacts of Inorganic PM_{2.5} and Precursor Emissions." *Atmospheric Environment* 137 (July): 80–89. <https://doi.org/10.1016/j.atmosenv.2016.04.026>.
- Hoesly, Rachel M., Steven J. Smith, Leyang Feng, Zbigniew Klimont, Greet Janssens-Maenhout, Tyler Pitkanen, Jonathan J. Seibert, et al. 2018. "Historical (1750–2014) Anthropogenic Emissions of Reactive Gases and Aerosols from the Community Emissions Data System (CEDS)." *Geoscientific Model Development* 11 (1): 369–408. <https://doi.org/10.5194/gmd-11-369-2018>.
- Jafino, Bramka Arga, Stephane Hallegatte, and Julie Rozenberg. 2021. "Focusing on Differences across Scenarios Could Lead to Bad Adaptation Policy Advice." *Nature Climate Change*, April, 1–3. <https://doi.org/10.1038/s41558-021-01030-9>.
- Jung, Jia, Yunsoo Choi, Seyedali Mousavinezhad, Daiwen Kang, Jincheol Park, Arman Pouyaei, Masoud Ghahremanloo, Mahmoudreza Momeni, and Hyuncheol Kim. 2022. "Changes in the Ozone Chemical Regime over the Contiguous United States Inferred by the Inversion of NO_x and VOC Emissions Using Satellite Observation." *Atmospheric Research* 270 (June): 1–14. <https://doi.org/10.1016/j.atmosres.2022.106076>.
- Kinney, Patrick L. 2018. "Interactions of Climate Change, Air Pollution, and Human Health." *Current Environmental Health Reports* 5 (1): 179–86. <https://doi.org/10.1007/s40572-018-0188-x>.

- . 2021. “How Can We Solve Our Air Quality Problem in the Face of Climate Change?” *JAMA Network Open* 4 (1): e2035010. <https://doi.org/10.1001/jamanetworkopen.2020.35010>.
- Li, Jianfeng, Yuhang Wang, and Hang Qu. 2019. “Dependence of Summertime Surface Ozone on NO_x and VOC Emissions over the United States: Peak Time and Value.” *Geophysical Research Letters* 46 (6): 3540–50. <https://doi.org/10.1029/2018gl081823>.
- Li, Ke, Daniel J. Jacob, Hong Liao, Jia Zhu, Viral Shah, Lu Shen, Kelvin H. Bates, Qiang Zhang, and Shixian Zhai. 2019. “A Two-Pollutant Strategy for Improving Ozone and Particulate Air Quality in China.” *Nature Geoscience* 12 (11): 906–10. <https://doi.org/10.1038/s41561-019-0464-x>.
- Monier, E., J. R. Scott, A. P. Sokolov, C. E. Forest, and C. A. Schlosser. 2013. “An Integrated Assessment Modeling Framework for Uncertainty Studies in Global and Regional Climate Change: The MIT IGSM-CAM (Version 1.0).” *Geoscientific Model Development* 6 (6): 2063–85. <https://doi.org/10.5194/gmd-6-2063-2013>.
- Monier, Erwan, Xiang Gao, Jeffery R. Scott, Andrei P. Sokolov, and C. Adam Schlosser. 2015. “A Framework for Modeling Uncertainty in Regional Climate Change.” *Climatic Change* 131 (1): 51–66. <https://doi.org/10.1007/s10584-014-1112-5>.
- Murray, Lee T. 2016. “Lightning NO_x and Impacts on Air Quality.” *Current Pollution Reports* 2 (2): 115–33. <https://doi.org/10.1007/s40726-016-0031-7>.
- Nam, Kyung-Min, Caleb J. Waugh, Sergey Paltsev, John M. Reilly, and Valerie J. Karplus. 2014. “Synergy between Pollution and Carbon Emissions Control: Comparing China and the United States.” *Energy Economics* 46 (November): 186–201. <https://doi.org/10.1016/j.eneco.2014.08.013>.
- Nguyen, Giang Tran Huong, Hikari Shimadera, Katsushige Uranishi, Tomohito Matsuo, and Akira Kondo. 2020. “Numerical Assessment of PM_{2.5} and O₃ Air Quality in Continental Southeast Asia: Impacts of Future Projected Anthropogenic Emission Change and Its Impacts in Combination with Potential Future Climate Change Impacts.” *Atmospheric Environment* 226 (April): 117398. <https://doi.org/10.1016/j.atmosenv.2020.117398>.
- Nolte, Christopher G., Tanya L. Spero, Jared H. Bowden, Megan S. Mallard, and Patrick D. Dolwick. 2018. “The Potential Effects of Climate Change on Air Quality across the Conterminous US at 2030 under Three Representative Concentration Pathways.” *Atmospheric Chemistry and Physics* 18 (20): 15471–89. <https://doi.org/10.5194/acp-18-15471-2018>.
- Nordhaus, William. 2014. “Estimates of the Social Cost of Carbon: Concepts and Results from the DICE-2013R Model and Alternative Approaches.” *Journal of the Association of Environmental and Resource Economists* 1 (1/2): 273–312. <https://doi.org/10.1086/676035>.
- Paltsev, Sergey, Erwan Monier, Jeffery Scott, Andrei Sokolov, and John Reilly. 2015. “Integrated Economic and Climate Projections for Impact Assessment.” *Climatic Change* 131 (1): 21–33. <https://doi.org/10.1007/s10584-013-0892-3>.
- Pommier, Matthieu, Hilde Fagerli, Michael Gauss, David Simpson, Sumit Sharma, Vinay Sinha, Sachin D. Ghude, Oskar Landgren, Agnes Nyiri, and Peter Wind. 2018. “Impact of Regional Climate Change

and Future Emission Scenarios on Surface O₃ and PM_{2.5} over India.” *Atmospheric Chemistry and Physics* 18 (1): 103–27. <https://doi.org/10.5194/acp-18-103-2018>.

Potts, Daniel A., Eloise A. Marais, Hartmut Boesch, Richard J. Pope, James Lee, Will Drysdale, Martyn P. Chipperfield, et al. 2021. “Diagnosing Air Quality Changes in the UK during the COVID-19 Lockdown Using TROPOMI and GEOS-Chem.” *Environmental Research Letters: ERL [Web Site]* 16 (5): 054031. <https://doi.org/10.1088/1748-9326/abde5d>.

Raes, Frank, Hong Liao, Wei-Ting Chen, and John H. Seinfeld. 2010. “Atmospheric Chemistry-Climate Feedbacks.” *Journal of Geophysical Research* 115 (D12). <https://doi.org/10.1029/2009jd013300>.

Rao, Shilpa, Zbigniew Klimont, Steven J. Smith, Rita Van Dingenen, Frank Dentener, Lex Bouwman, Keywan Riahi, et al. 2017. “Future Air Pollution in the Shared Socio-Economic Pathways.” *Global Environmental Change: Human and Policy Dimensions* 42 (January): 346–58. <https://doi.org/10.1016/j.gloenvcha.2016.05.012>.

Reis, Lara Aleluia, Laurent Drouet, and Massimo Tavoni. 2022. “Internalising Health-Economic Impacts of Air Pollution into Climate Policy: A Global Modelling Study.” *The Lancet. Planetary Health* 6 (1): e40–48. [https://doi.org/10.1016/S2542-5196\(21\)00259-X](https://doi.org/10.1016/S2542-5196(21)00259-X).

Schneidmesser, Erika von, Charles Driscoll, Harald E. Rieder, and Luke D. Schiferl. 2020. “How Will Air Quality Effects on Human Health, Crops and Ecosystems Change in the Future?” *Philosophical Transactions. Series A, Mathematical, Physical, and Engineering Sciences* 378 (2183): 20190330. <https://doi.org/10.1098/rsta.2019.0330>.

Schultz, Martin G., Sabine Schröder, Olga Lyapina, Owen Cooper, Ian Galbally, Irina Petropavlovskikh, Erika Von Schneidmesser, et al. 2017a. “Tropospheric Ozone Assessment Report: Database and Metrics Data of Global Surface Ozone Observations.” *Elementa (Washington, D.C.)* 5 (0): 58. <https://doi.org/10.1525/elementa.244>.

Schultz, Martin G., Sabine Schröder, Olga Lyapina, Owen R. Cooper, Ian Galbally, Irina Petropavlovskikh, Erika von Schneidmesser, et al. 2017b. “Tropospheric Ozone Assessment Report, Links to Global Surface Ozone Datasets.” PANGAEA - Data Publisher for Earth & Environmental Science. <https://doi.org/10.1594/PANGAEA.876108>.

Soest, Heleen L. van, Detlef P. van Vuuren, Jérôme Hilaire, Jan C. Minx, Mathijs J. H. M. Harmsen, Volker Krey, Alexander Popp, Keywan Riahi, and Gunnar Luderer. 2019. “Analysing Interactions among Sustainable Development Goals with Integrated Assessment Models.” *Global Transitions* 1 (January): 210–25. <https://doi.org/10.1016/j.glt.2019.10.004>.

Sofiev, Mikhail, James J. Winebrake, Lasse Johansson, Edward W. Carr, Marje Prank, Joana Soares, Julius Vira, Rostislav Kouznetsov, Jukka-Pekka Jalkanen, and James J. Corbett. 2018. “Cleaner Fuels for Ships Provide Public Health Benefits with Climate Tradeoffs.” *Nature Communications* 9 (1): 406. <https://doi.org/10.1038/s41467-017-02774-9>.

Tessum, Christopher W., Jason D. Hill, and Julian D. Marshall. 2017. “InMAP: A Model for Air Pollution Interventions.” *PLoS One* 12 (4): e0176131. <https://doi.org/10.1371/journal.pone.0176131>.

Vohra, Karn, Alina Vodonos, Joel Schwartz, Eloise A. Marais, Melissa P. Sulprizio, and Loretta J. Mickley. 2021. "Global Mortality from Outdoor Fine Particle Pollution Generated by Fossil Fuel Combustion: Results from GEOS-Chem." *Environmental Research* 195 (April): 110754. <https://doi.org/10.1016/j.envres.2021.110754>.

Westervelt, D. M., C. T. Ma, M. Z. He, A. M. Fiore, P. L. Kinney, M-A Kioumourtzoglou, S. Wang, J. Xing, D. Ding, and G. Correa. 2019. "Mid-21st Century Ozone Air Quality and Health Burden in China under Emissions Scenarios and Climate Change." *Environmental Research Letters: ERL [Web Site]* 14 (7): 074030. <https://doi.org/10.1088/1748-9326/ab260b>.

Supplemental information: Rapid estimation of climate-air quality interactions in integrated assessment using a response surface model

Sebastian D. Eastham^{1,2}, Erwan Monier^{2,3}, Daniel Rothenberg², Sergey Paltsev², Noelle E. Selin^{2,4,5}

¹Laboratory for Aviation and the Environment, Massachusetts Institute of Technology, Cambridge, MA 02139

²Joint Program on the Science and Policy of Global Change, Massachusetts Institute of Technology, Cambridge, MA 02139

³Land, Air and Water Resources, University of California Davis, Davis, CA 95616

⁴Institute for Data, Systems, and Society, Massachusetts Institute of Technology, Cambridge, MA 02139

⁵Department of Earth, Atmospheric, and Planetary Science, Massachusetts Institute of Technology, MA 02139

*Correspondence to: seastham@mit.edu

Processing of TOAR-I data and evaluation of ozone in GCHP-CAM

We downloaded all available data from the TOAR-I archive on July 14th 2022. As shown in Figure S1, most TOAR-I contributor sites are found in North America and Europe, although there are a small number outside this region.

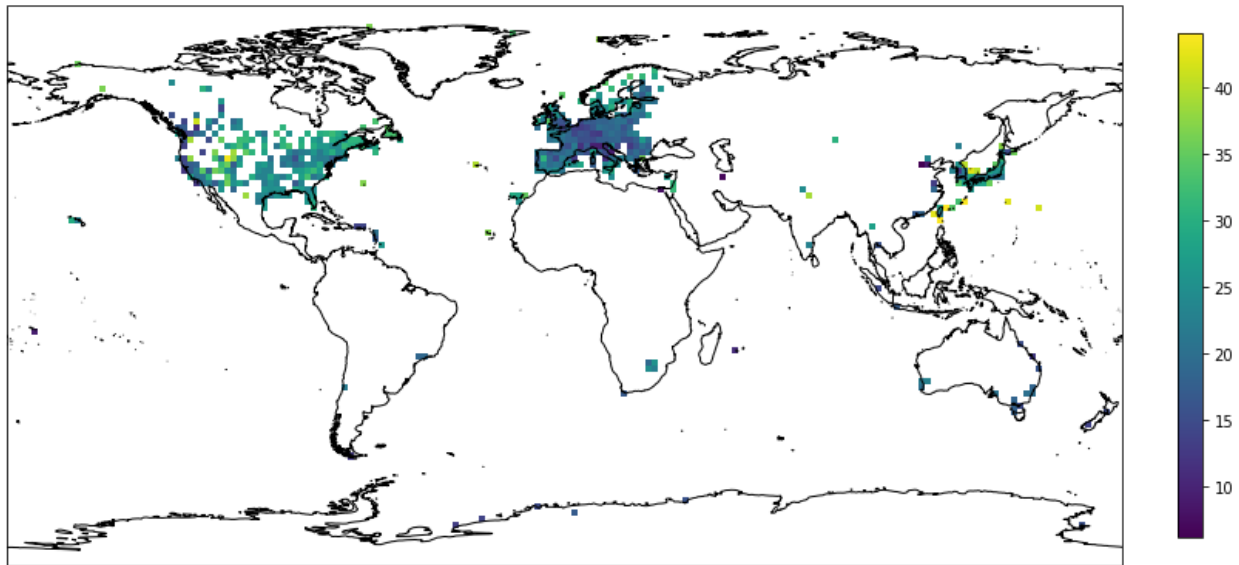


Figure S1. Sites from the TOAR-I database used for evaluation of surface ozone. Annual mean ozone in ppbv is shown using color.

For comparison to results from GCHP, we take the average of all $2^{\circ} \times 2^{\circ}$ TOAR-I grid cells (reporting observations from 2010-2014) within each GCHP grid cell. This avoids the introduction of bias through comparing the same model result to multiple sites, while also somewhat reducing the dominance of North American and European sites in the dataset. A comparison of the annual mean values (using only TOAR-I averaging cells which reported data for all 12 months) is shown in Figure S2, with a brief analysis provided in the main text.

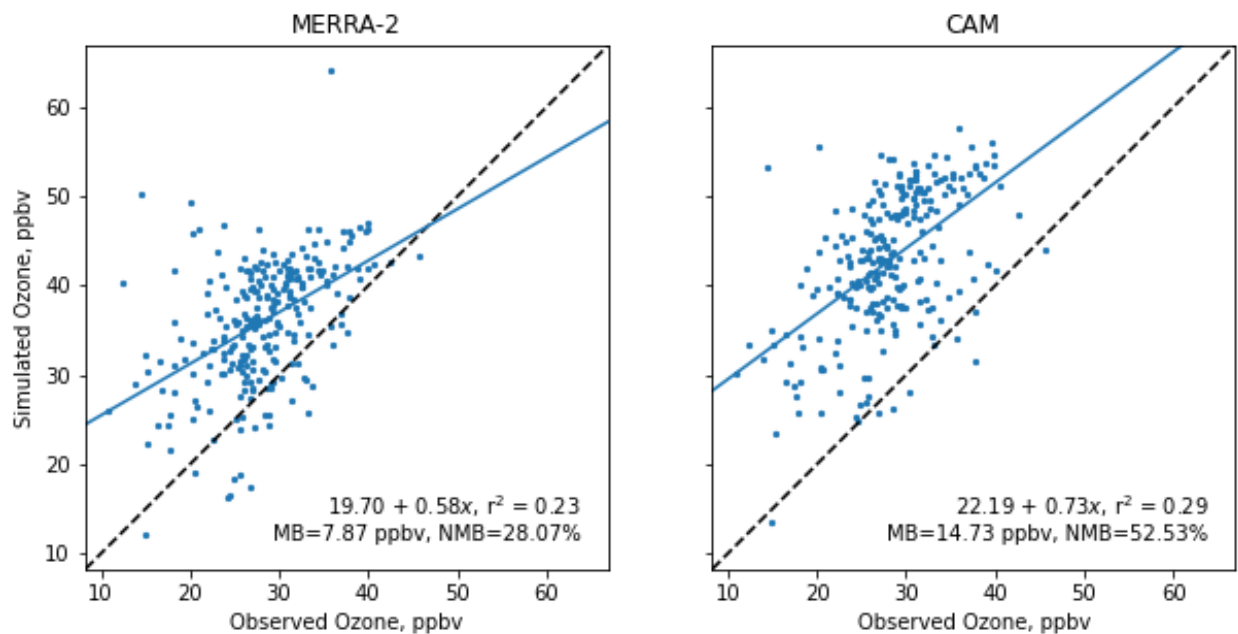


Figure S2. Comparison of observed surface ozone (2010-2014 inclusive, averaged) to the annual mean for 2014 calculated using GCHP. Left panel: comparison to simulations using reanalysis meteorology from MERRA-2. Right: comparison to simulations using meteorological data from the CAM “pol3.7” simulation (single ensemble member).

We apply the same procedure to calculate r^2 for each month of the year. The result is shown in Figure S3. The CAM-driven simulation achieves an r^2 equal or greater than that from the MERRA-2-driven simulation for 8 of 12 months. However, the mean bias is consistently greater.

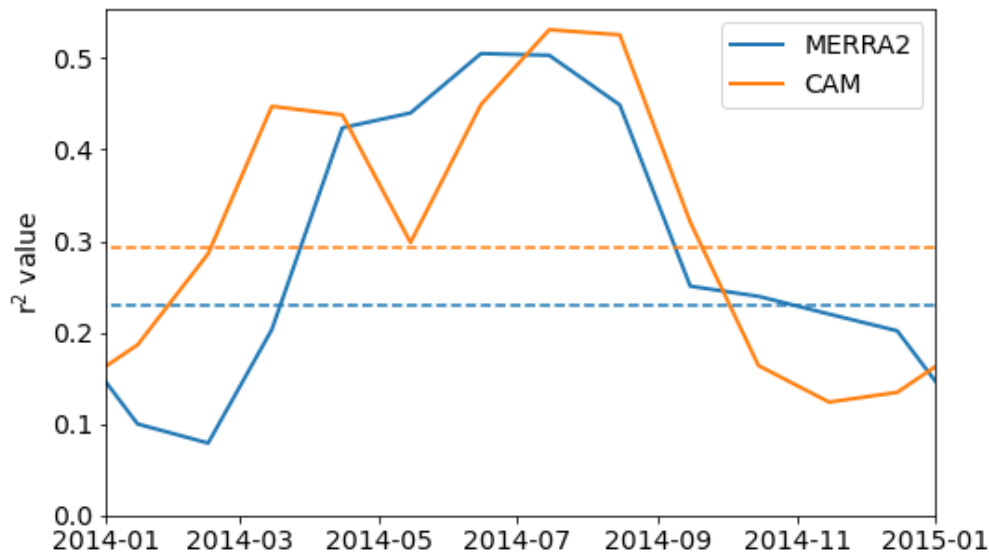


Figure S3. Month-by-month evaluation of the correlation between observed surface ozone (from TOAR-I, for 2010-2014 averaged) and simulated surface ozone. Dashed lines show the annual average value.

Evaluation of wet deposition in GCHP-CAM

In addition to the evaluation of surface ozone, we also evaluate the representation of wet deposition in GCHP. Since wet deposition is a key removal mechanism for ozone precursors as well as fine particulate matter (PM_{2.5}), a reasonable representation of wet deposition is important. We compare observed rates of wet deposition (Vet et al., 2014) of SO₄ (in kgS/ha/yr) and NO₃ (kgN/ha/yr) to removal rates from GCHP. As in the case of ozone, removal rates are averaged across sites in the same cells. This reduces the number of sites from 484 (see Figure S4) to 201.

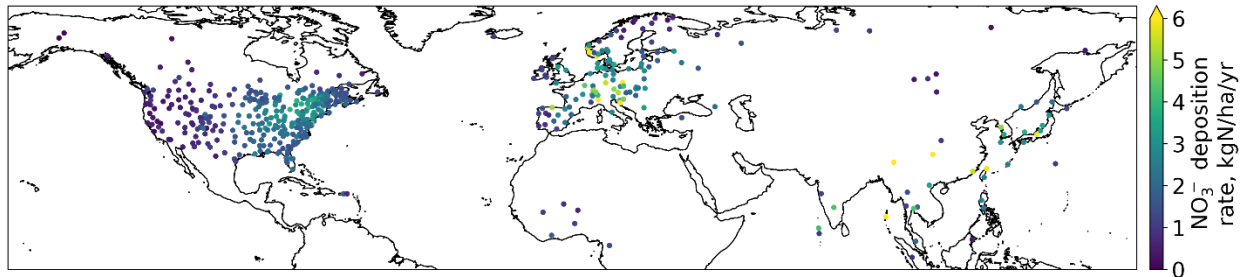
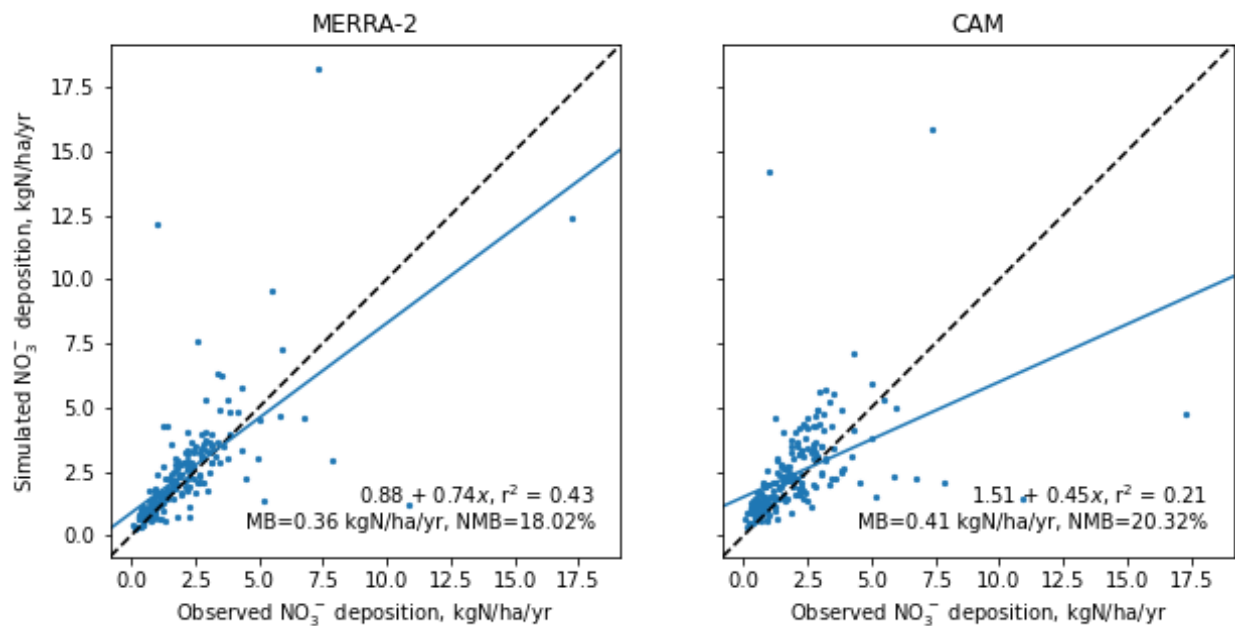


Figure S4. Sites from Vet et al. (2014) used for evaluation of wet deposition. Annual mean nitrate wet deposition rate is shown using color.

A comparison of observed and simulated removal rates is shown in Figure S5. Simulations using CAM show reduced skill in simulating nitrate aerosol, with a reduced r^2 of 0.21 compared to 0.43 when using MERRA-2. However, the normalized mean bias is similar (20% compared to 18% with MERRA-2). The model's skill in simulating sulfate removal is largely unchanged (r^2 of 0.63 in CAM, compared to 0.61 in MERRA-2). Although both simulations show a bias greater than -50%, this is likely due to the dataset being generated from data for 2005-2007. Emissions of SO₂ in are estimated to have fallen globally between 2006 and 2014 by 23%, and by 59% in the US specifically (McDuffie et al., 2020).



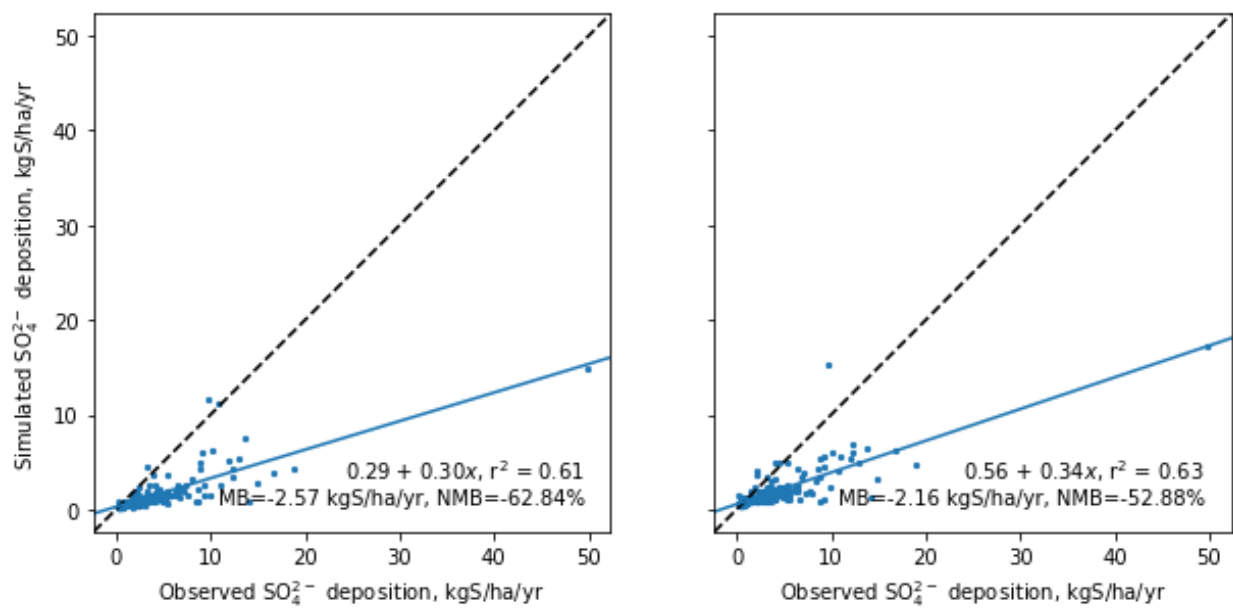


Figure S5. Comparison of observed (x-axis) and simulated (y-axis) removal rates for nitrate (top row) and sulfate (bottom row). Left column: comparisons using MERRA-2 reanalysis data as meteorological input. Right column: comparisons using CAM-generated data (this study) as meteorological input.

References

- McDuffie, E. E., Smith, S. J., O'Rourke, P., Tibrewal, K., Venkataraman, C., Marais, E. A., Zheng, B., Crippa, M., Brauer, M., and Martin, R. V.: A global anthropogenic emission inventory of atmospheric pollutants from sector- and fuel-specific sources (1970–2017): an application of the Community Emissions Data System (CEDS), *Earth Syst. Sci. Data*, 12, 3413–3442, 2020.
- Vet, R., Artz, R. S., Carou, S., Shaw, M., Ro, C.-U., Aas, W., Baker, A., Bowersox, V. C., Dentener, F., Galy-Lacaux, C., Hou, A., Pienaar, J. J., Gillett, R., Forti, M. C., Gromov, S., Hara, H., Khodzher, T., Mahowald, N. M., Nickovic, S., Rao, P. S. P., and Reid, N. W.: A global assessment of precipitation chemistry and deposition of sulfur, nitrogen, sea salt, base cations, organic acids, acidity and pH, and phosphorus, *Atmos. Environ.*, 93, 3–100, 2014.